

Addressing Energy Forecast Errors – An Empirical Investigation of the Capacity Distribution Impact in a Variable Storage

Dejan Ilić · Stamatīs Karnouskos

Manuscript available at <http://dx.doi.org/10.1007/s12667-014-0119-3>

Abstract Today energy load forecasting is used by retailers to predict their future energy needs and address them in cost-effective ways. However, with the prevalence of the smart grid, accurate forecasting is becoming increasingly important, as the stakeholder base expands and differentiates by transforming to active prosumers who make their own forecasting and take advantage of the new smart grid capabilities for addressing excess or shortage of energy. For instance, they can benefit from participation in demand-response programs, or more futuristic such as local energy marketplaces. To take advantage of such opportunities, controllable energy signature in order to gain predictability is of key importance. We present here an empirical approach towards understanding how the predictability of a stakeholder can be improved through the availability of variable storage. The guiding question is to investigate the relevance of capacity sizing for absorption of the intra-day forecast errors. The increase of variable storage in existing facilities such as that offered by the presence of electric vehicles in a building's charging stations, poses new potentially cost-effective ways that facility managers can consider in the effort to maintain control of their infrastructure's energy signature. Here we show, in a step-by-step approach, how intra-day energy forecast errors of a building, impact the overall capacity variation required to absorb them, and how proper storage shaping can assist. Although the approach is empirical, the same steps may be applied in other similar cases.

Keywords Smart metering · building energy prediction · storage estimation

1 Introduction

Forecasting plays a pivotal role in facility management processes, strategic planning, and business strategy. Its implications range from technical aspects, where the quality of service has to be guaranteed, to business aspects, with impact on budget, strategy and other enterprise goals such as efficiency, sustainability, corporate social responsibility etc. Increasing technology usage in modern buildings [1] enables innovative approaches to be engaged that provide accurate behaviour of the energy signature of a building [2].

The increase in dynamic usage of the building's resources makes the goal of a predictable behaviour challenging [3]. Being able to predict accurately the energy signature may benefit not only internal facility management processes, but also empower visionary scenarios of the smart grid, where buildings can be active participants within city-wide energy management schemes such as demand-response and future energy markets [4, 5]. The latter may act as an enabler for new business opportunities for facility managers including the emerging roles of the smart grid stakeholders [6], and benefit potential optimization at more global level and not only on the specific facility in question.

Today, due to the limited communication among the grid stakeholders (e.g. grid managers and consumers), their multi-level aggregation is used to reduce imbalances of inaccurate load forecasts [7]. However, with the emergence of the smart grid and its detailed monitoring offered [8], one can work on fine-grained data and better understand individuals and their impact to the forecasting process, such that benefits of having them predictable can be assessed [9]. In some examined cases, using aggregation to improve forecast accuracy was found to converge rapidly [10]. In addition storage technologies were identified as a key enabler to a rapid convergence of a cluster [11].

The behaviour of stakeholders and accuracy of their forecast plays a pivotal role in the required storage capacity that would be needed to balance the excess or shortage of energy over time. As it can be seen in Figure 1, the difference in energy consumption of a commercial building indicates that same accuracy in peak times will need more storage capacity to absorb errors. Using on premise available energy storage, could help towards enhancing its predictability, such that "sufficient accuracy" is achieved [12].

As storages already play a key role in future energy management scenarios [13], their technological limitations are already well known [14]. In this work we propose a simple method to estimate storage capacity needs required to absorb the induced errors. While we don't really consider any specific storage technology here, we have in mind that many battery-based approaches are still expensive for most grid storage applications [15]. Hence we stay at high level with respect to the actual storage characteristics, and benefit that our approach can also be applied with existing assets, such as a fleet of company electric cars [2]. The interest on the later is that (i) will be available in high numbers in the future and are still company-owned assets whose management can be realized together with the facility management goals, and (ii) they offer a variable storage capability depending on their availability and usage

patterns. With that in mind, it is expected that capacity need to absorb forecasting errors will significantly vary within the intra-day intervals.

We approach this use-case in an empirically, depending on the smart metering data of a commercial building and in a step-by-step way we incrementally show its applicability. We aim at understanding how important is storage capacity for the absorption of forecasting errors especially in the highly volatile intra-day energy loads. Once the impact is understood, one may use such knowledge to propose “solution shapes”, i.e. timeline of the quantity of storage needed to improve prediction of stakeholders. The evaluation will show a case where different shaping of the storage can significantly reduce the overall capacity needed. The actual impact of a specific technology as well as other side-effects on business or financial aspects are left for future work.

2 Energy Signature of a Commercial Building

Electricity consumers have different consumption patterns, and for commercial buildings one can witness significant variations over workdays, weekends and holidays as seen in [Figure 1](#) and [Figure 2](#). Both figures are derived from smart metering data of a commercial building collected throughout 2011 in the region of Baden-Württemberg, Germany. The building has 139 offices, mainly used between 08:00–17:00, with total measured consumption of approximately $2.7GWh$ for 2011.

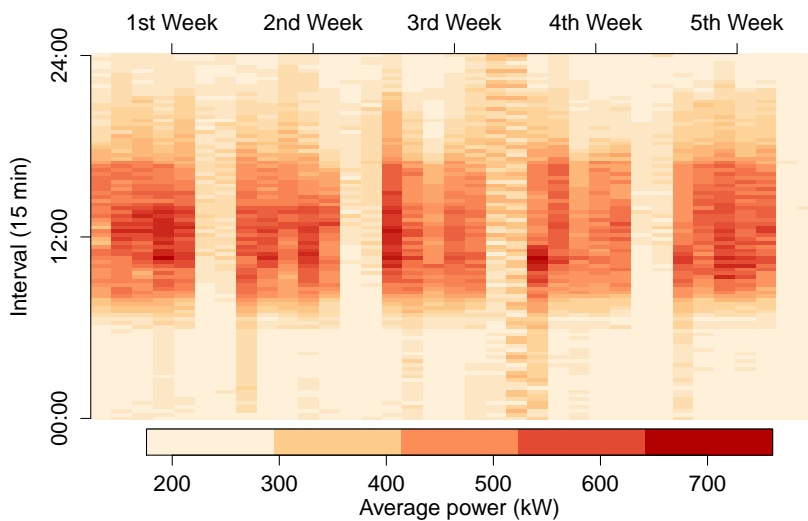


Fig. 1 Heatmap of energy consumption of a commercial building

In [Figure 1](#) data for 5 weeks is depicted; however we can already notice the variations during the day and especially near noon. Such variations repeat continuously over the entire year. [Figure 2](#) provides a clearer view on the

average daily power for both, workdays and weekends. As expected there is significant difference in building's average power needs based on day of a week. In particular, the average demand for workdays is ≈ 340 kW and ≈ 210 kW over the weekend. On daily average, workday consumption is 56% greater than weekends, resulting to (a yearly consumption over workdays) 4 times greater than the total weekend consumption. This is important to notice, due to the potential of improving the building's predictability over the weekdays where storage sizing needed can drastically variate.

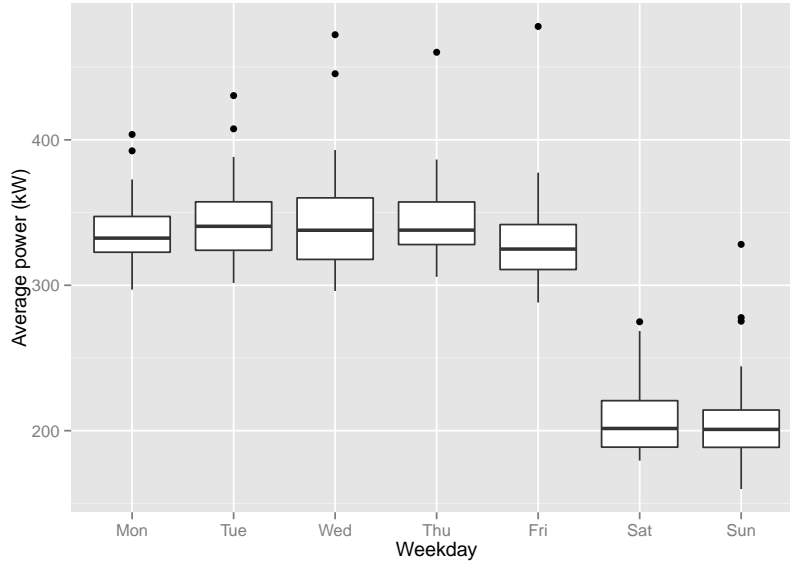


Fig. 2 Daily average power for workdays and weekends

Such significant differences on the behaviour, will result in a separation to different sets. The main set D containing all days, will be divided to two subsets, D_w and D_e for workdays and weekends respectively. Additionally, a significant consumption variation is expected from high intra-day variations, what also can be noticed in [Figure 1](#). To better understand its impact, a view of the average daily 15-minute intervals over the two created datasets is shown on [Figure 3](#).

The curve depicted shows the impact of building's processes for preparation of the workday, and the impact of employees arriving at the office as well as the actual usage of it during office hours. The drop seen is also expected after the leave of employees from the facilities and conclusion of other tasks (cleaning, maintenance etc.) which lead to an almost minimum operational level after approx. 21:00 (which is where the two curves of weekdays and weekends converge). The observation on the intra-day load difference between the two sets (D_w and D_e) is expected to give an initial answer to how capacity

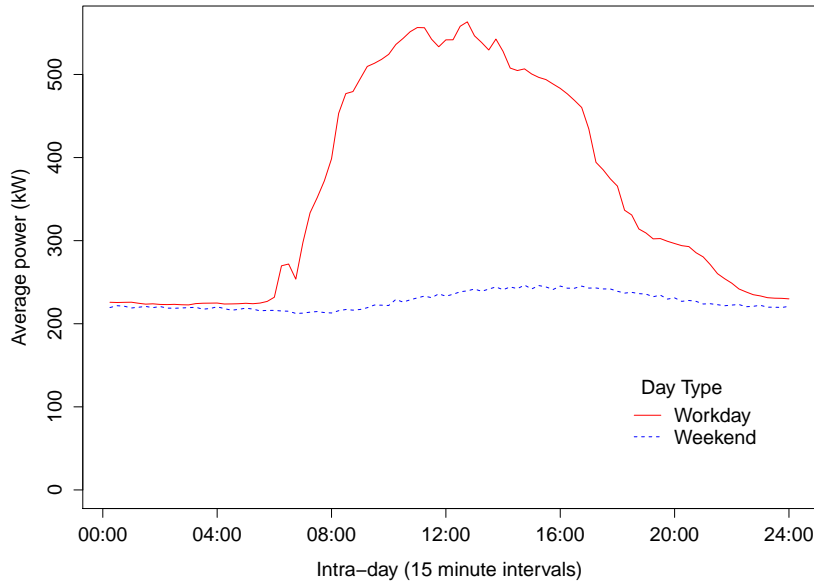


Fig. 3 Average power (kW) per interval averaged over entire year

need variates based on the load. Although the empirical analysis in this work involves only the load of a specific commercial building, the same methodology may be followed also in other use-cases.

3 Predictability Assessment

Although several forecast approaches [16, 17] could be applied to the consumption data collected from the building, we decided to use the Seasonal AutoRegressive Integrated Moving Average (SARIMA) model, which can be used to predict electricity demand [18]. The weekly seasonality is considered and 4 seasons are used to train the model. The days of January 2011 were not predicted, and therefore are not included. To differentiate, the subset of days of the original set D (without January) is noted as D' .

Energy consumption is represented as series of intervals n (in this case of 15 minutes) and the series length is denoted as l . The actual energy consumed within an interval is denoted as $y[n] \geq 0$, where $n \in [1, l]$. The consumption forecasting is made for a short-term horizon, in particular for one day ($l = 96$), and the forecast interval is denoted as $\hat{y}[n] \geq 0$. Forecast accuracy is usually measured by Mean Absolute Percentage Error (MAPE), however in this work we primarily focus on the absolute energy difference between forecast and actual consumption (which is responsible for the storage sizing later discussed in section 4). If a forecast error (in kWh) of an interval is calculated as $w[n] =$

$\hat{y}[n] - y[n]$, the total absolute error over one particular day is calculated as $w_{tot} = \sum_{n=1}^l |w[n]|$.

The building's energy signature highly depends on the usage pattern e.g. by the employees who are active during the week but absent during the weekends. By using the SARIMA model, the forecast error w_{tot} for the building was evaluated and Figure 4 visualizes the w_{tot} for different weekdays in D'_w and D'_e over the entire year. This result can be considered as an initial clue to the relevance of the available capacity on daily basis.

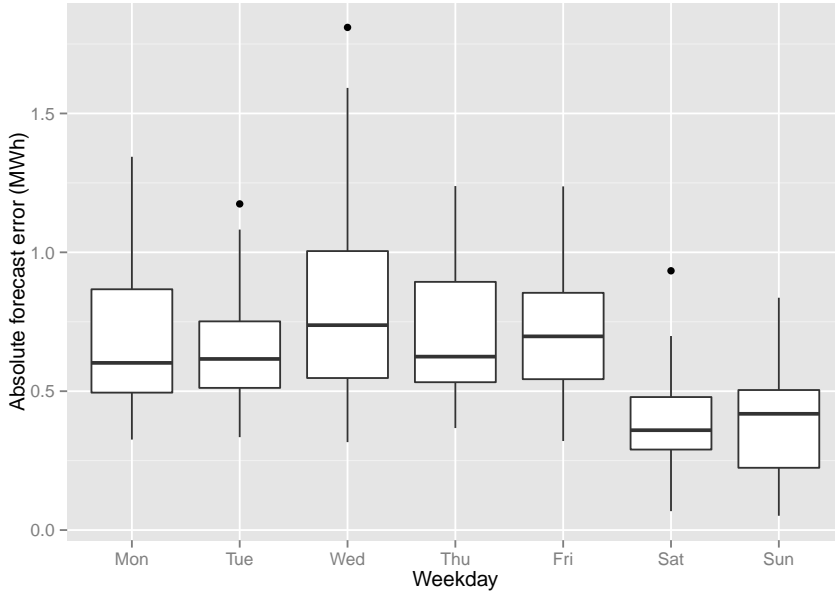


Fig. 4 Daily absolute energy error on weekdays over the entire set

As it can be seen, forecast errors over workdays (D'_w) result in a higher error. Greater consumption over the workdays (as indicated in Figure 2), correlates to greater absolute forecast errors in Figure 4. We have to note that although some samples of the two datasets resulted in a greater forecast error, it is hard to identify the exact origin of the error in those particular samples. One may attribute these to the potentially stochastic behaviour of the employees e.g. such as vacation period, or working outside the office hours. However, in the effort of identifying the source of forecast errors we should consider also the behaviour from Figure 3; hence some analysis need to be applied for the forecast errors. In Figure 5 one can see the intra-day effect of every 15 minute interval n , averaged over the workdays $\langle |w[n]| \rangle_{D'_w}$ and weekends $\langle |w[n]| \rangle_{D'_e}$.

As depicted in Figure 5, the time of the day highly impacts the difference in quantity of the forecasting error (in kWh). At the begin (of the averaged

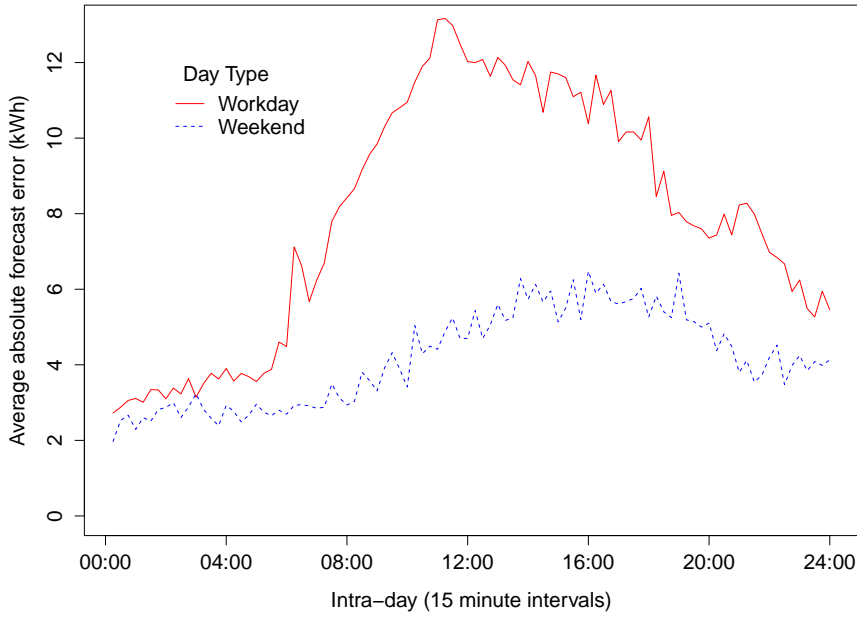


Fig. 5 Absolute forecast error averaged over intervals to identify intra-day origin of the error

series) workdays and weekends have a comparable forecast error, however the error w_{tot} for the midday of workdays increases significantly. On a closer look, we can identify that some intervals of workdays have 3-fold or 4-fold greater errors than other intervals. Although we can not clearly identify the source of the error, we can see the correlation of it with the employee working hours (and potentially other processes that relate to them). This intra-day variation of the error is expected to impact the variable storage requirement. This coincides with what we concluded from the quantitative daily variation in [Figure 4](#). Hence it will be further investigated in [section 6](#).

4 Analysis Approach

Uncertainty of the prediction algorithm applied in [section 3](#), affects the propagation of the forecast error to the storage capacity demand and need to be considered for variable sizing. Others identified similar behaviour [\[19\]](#), however due to the availability of the real-world data from [section 2](#), the storage that would be sufficient can be directly measured (a posteriori).

The difference between the forecast and actual consumption is noted as $w[n]$. A positive value indicates a surplus, and a negative one a shortage. A simple cumulative function of individual forecast errors from each interval $n \in [1, l]$ is used as the estimation method. [Figure 6](#) represents an example of estimating the storage capacity c_e as from the sum of $w[n]$ for one day. The actual

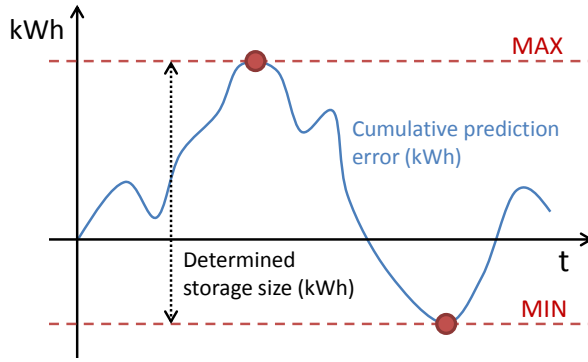


Fig. 6 Determination of an ideal storage capacity to address errors of a daily prediction

distance between the function extremes is used as the indicator. If a set of cumulative forecast errors is presented as $w_{cum} = \{w[1], \sum_{n=1}^2 w[n], \dots, \sum_{n=1}^l w[n]\}$, then the estimated storage size is calculated as $c_e = \max(w_{cum}) - \min(w_{cum})$. This method returns the optimal sizing for each day individually. The approach shortly depicted here is further used for the investigations described in [section 5](#) and [section 6](#).

5 Storage Capacity Estimation

The evaluation of the building data observed in [section 2](#) is done according to the storage estimation approach presented in [section 4](#). One day of the original energy consumption is represented as $l = 96$ of 15 minute intra-day intervals and for the following experiments the same resolution is used. The forecast model is trained with four weeks of meter reading data of the same interval resolution under the constraints already discussed in [section 3](#).

[Figure 7](#) depicts an initial indication on estimated storage size (and their average), for each day from the two considered datasets. There, one can see the variation in storage needs imposed by the weekdays. The weekend dataset D'_e had clearly lower consumption (as shown in [Figure 2](#)) and understandably result in a lower storage requirement c_e . The average estimated storage for workdays is approx. $\langle c \rangle_{D'_w} \approx 475kWh$, requiring almost double the storage in comparison to $\langle c \rangle_{D'_e} \approx 305kWh$. Although is not straightforward in [Figure 7](#), one can still see that the average required storage capacity $\langle c_e \rangle_{D'_w}$ is covering approximately 95% of the estimated storage size $\langle c_e \rangle_{D'_e}$. The resulting average estimation from [Figure 7](#) is the second clue of the needed variable capacity.

The percentage of daily energy consumed and the estimated storage size also need to be better understood, in order to understand the storage's impact to predictability. Based on the results obtained from [Figure 7](#), the estimated capacities of both sets are represented by the cumulative density function in [Figure 8](#). If results are observed as percentages, the mean estimated storage

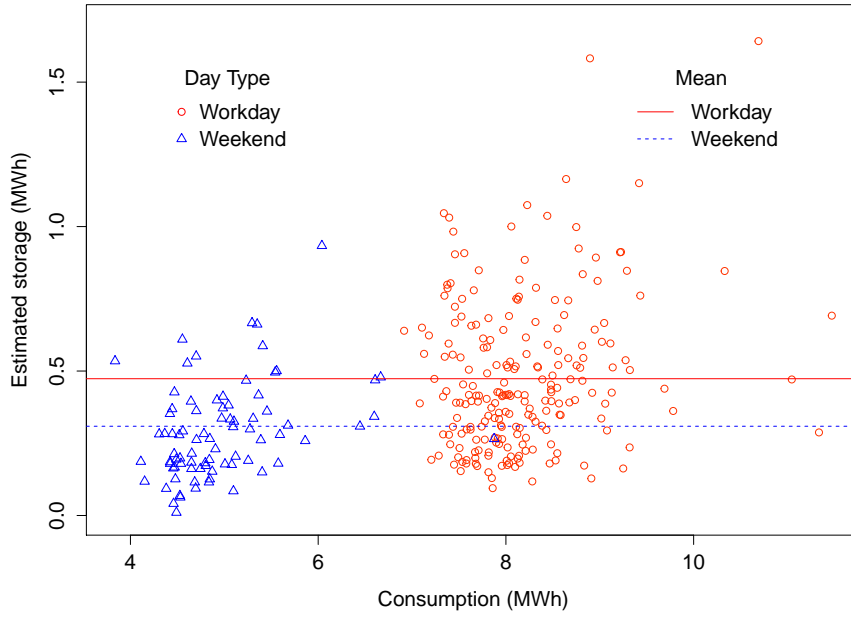


Fig. 7 Storage size estimation for consumed energy (within a day)

size is covered with only 6, 4% of workday and 5, 5% of weekend consumption. Interestingly most of the forecast error is covered with a storage size of 10% of the individual daily consumption. Approximately 92% of the forecast error in D'_e can be covered by the capacity of 10% the consumption, while the capacity of 14% the consumption covers entirely the incurred error. Workdays are $\approx 83\%$ covered by c_e sizing 10% of daily consumption. With 15% of the consumption, 97% of the set can be covered. Finally with storage equaling to 18% of daily consumption, the entirely generated error can be absorbed.

A few estimations showed a greater capacity requirement, as depicted in Figure 7 for both sets. Their origin should be more closely investigated prior to taking any decisions in a real-world storage deployment. The continuous distance increase between the two datasets can also be noticed and its origin will be further investigated in section 6.

6 Variable Storage Capacity

Many factors can impact the efficient capacity sizing, including the accuracy of a forecasting algorithm. In the case discussed in this work, the usage of the SARIMA algorithm resulted in the higher accuracy (in comparison to the Seasonal Naïve algorithm evaluated in [10]). However, we are aware that further improvements may be made by tweaking of the parameters or further processing statistically the data set, which however are seen as the core of this work. Although SARIMA resulted with an average MAPE of 8.2%, the high

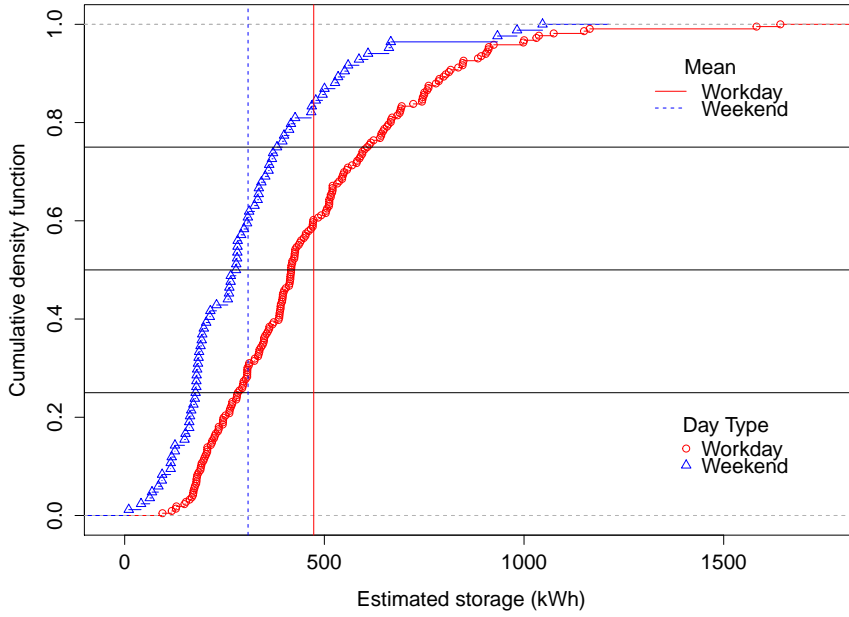


Fig. 8 Distribution of the estimated storage from daily estimations

propagation of the forecast errors had a significant impact on the resulting estimations. As such, the extracted c_e from the applied estimation method should be observed through its efficiency as depicted in Figure 9. The re-usage average (of the daily estimated storage) resulted similar for workdays $\langle \frac{w_{tot}}{c_e} \rangle_{D'_w} \approx 169\%$ to that of the weekend $\langle \frac{w_{tot}}{c_e} \rangle_{D'_e} \approx 152\%$. Figure 9 shows low re-usage for most of the samples, while certain days did result in a high re-usage rate, e.g. 250%.

Since reusing of storage capacity was identified as low (in Figure 9), the origin for the storage requirement due to absorption of the forecast errors gains importance. Identifying how the error propagates within a day, will help to better understand the role of the variable storage shape over time. The absolute forecast error presented in section 3 may also lead to definition of an adequate shape. Some instances in Figure 5 resulted in greater forecast errors, but it is not clear how they mostly propagate to the resulting storage estimations c_e . Hence, the estimation method discussed in section 5 is used on intra-day intervals, in order to assess their individual impact to the overall storage estimated in the day they occur.

Based on the slope variation in Figure 3, it was decided to estimate the requirements c_e^x for six intra-day intervals (4-hour each). The impact of each interval ($x \in [1, \dots, 6]$) is calculated as $\frac{c_e^x}{c_e}$, where c_e^x and c_e occur during the same day. Such impact is evaluated for all days (for both D'_w and D'_e sets) and depicted in Figure 10. As it can be seen, certain intra-day intervals have much higher impact than others, e.g. as high as threefold impact. For evaluation

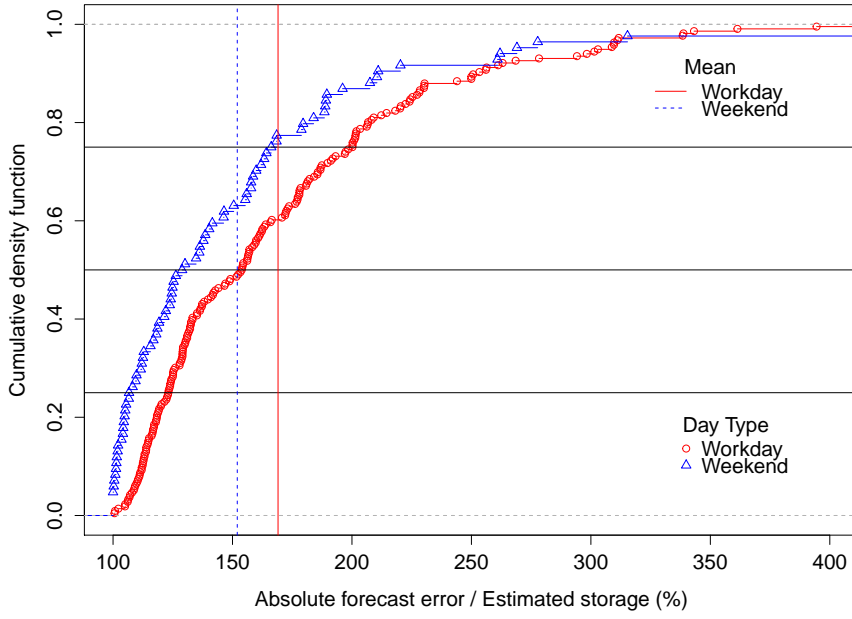


Fig. 9 Per day efficiency of the daily estimated storage in absorbing the forecast error by its re-usage

of the workday dataset, the estimated capacities c_e are mostly inflated by midday intervals, in particular from 08:00–12:00, 12:00–16:00, and 16:00–20:00 intervals. The results depicted in [Figure 10](#) assist towards understanding the storage distribution relevance on intra-day basis. Therefore, the continuous dynamic adjustment of the storage availability [19] should be considered even for intra-day intervals.

Comparing [Figure 7](#) and [Figure 10](#) we can conclude that requirements for storage sizing can be further reduced if the total capacity of a storage is properly distributed. These two figures suggest further focus on key intra-day intervals of a variable storage to absorb the error. To further investigate this, the capacities available within the intra-day intervals variate over time, respecting the overall shape of the variable storage. As such, the D'_w set is used to validate the hypothesis, where integrals of shapes presented in [Figure 11](#) equal to the each other. If the capacity shape functions are indicated as $c_i[n]$ and $c_j[n]$, dependency is described as:

$$\sum_{n=1}^l c_i[n] \equiv \sum_{n=1}^l c_j[n] \quad \forall i, j, \quad (1)$$

for all the intervals of a day, where i and j are the shape identifiers. The shapes for the variable storages hereby are selected as: (i) constant, (ii) identified peak and all intervals from [Figure 10](#), and (iii) finally the actual error measured in [Figure 5](#) for D'_w . It should be noticed that the capacity shapes $c_i[n]$ are

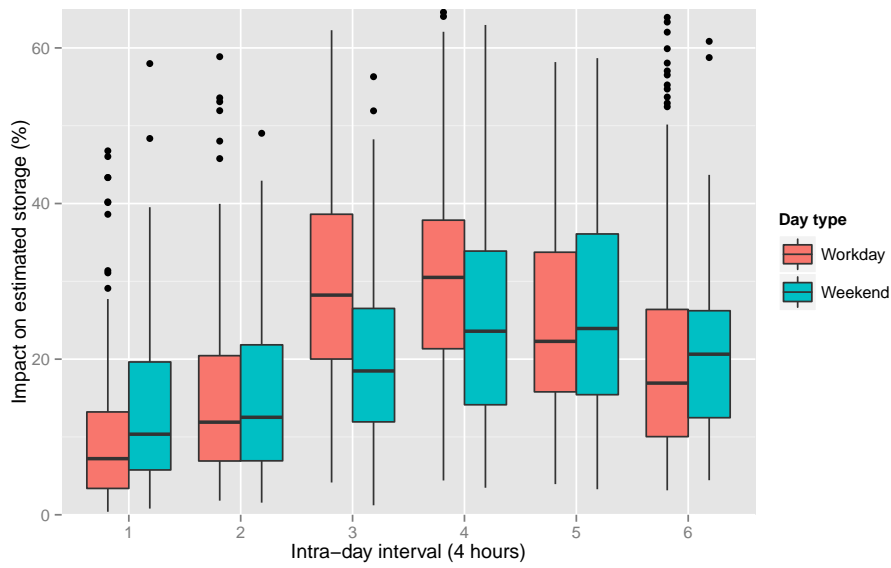


Fig. 10 Impact of intra-day intervals to the storage requirements

percentages and their final sizing is based on the total variable capacity c . For example, the constant shape will always have c value, while the peak function will either have 0 kWh or $2 * c$ kWh available for an interval n .

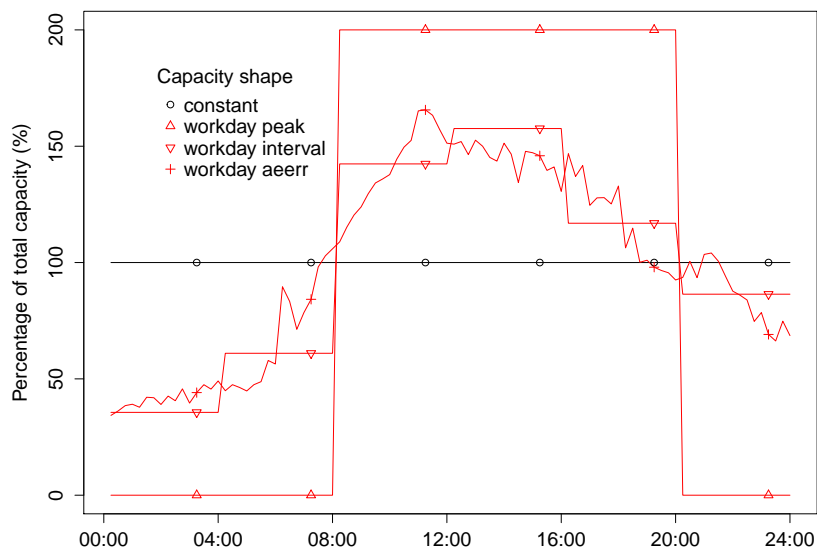


Fig. 11 Shapes for a variable storage capacity for intra-day intervals based on experiments for D'_w

To measure the efficiency of the each storage shape proposed in [Figure 11](#), the methodology detailed in [\[11\]](#) is adopted for charging and discharging behaviour. Hence charging/discharging efficiency of a specific storage technology is not considered and $w[n]$ is absorbed if the storage can absorb it (based on its state of charge). A variable storage introduces an increased complexity of unit management, in particular towards estimating the connection and disconnection State of Charge (SOC) of an individual asset [\[20\]](#), which is not addressed in this work. SOC cannot be treated individually (based on an asset), and if $n_1 < n_2$, the overall SOC of the storage is expressed as

$$SOC[n_2] = \frac{SOC[n_1]c[n_1] + a(c[n_2] - c[n_1])}{c[n_2]}, \quad (2)$$

where state at n_2 is inherited by its previous condition (at n_1) and forecast error is added. As the SOC per unit is not available, the variable a is introduced for the overall SOC over time. For the cases in this work, variable a is considered as

$$a = \begin{cases} 50\%, & c[n_2] \geq c[n_1] \\ SOC[n_1], & \text{otherwise.} \end{cases}$$

Following this setup, every shape from [Figure 11](#) is evaluated individually for the entire day and the resulting MAPE is averaged to understand its overall impact. With [Equation 1](#) one can directly compare efficiency of different shapes (to address errors of a forecast algorithm) only by varying the overall storage capacity c . In the following experiment c is set as a percentage of the average daily consumption. Hence, 2% of storage capacity is calculated as $c = (2.7\text{GWh}/365) * 0.02 \approx 145\text{kWh}$. By considering the D'_w set and other values of c , the verification of the assumption for the proposed shapes is illustrated in [Figure 12](#).

Although the peak shape had a fast convergence rate, it converges towards a $MAPE > 0\%$. This was somehow expected, as many intervals in the shape had $c_i[n] = 0\%$ of the total capacity c . The constant storage resulted in high drop for low capacities, while almost linear drop is noticed for $c \geq 4\%$. The interval based capacities had a slightly better performance, however the shape of capacity from [Figure 5](#) was highly efficient. The impact of having the capacity distributed as absolute energy error (or “aeerr” in the figure) may pose as a reliable indicator of where the focus should be on the effort to improve efficiency of a storage. It is critical to note the indications of [Figure 12](#), where even the slightest variation of the capacity distribution provoked a significant improvement to the overall performance. As an example, in [Figure 12](#) it can be seen that the MAPE for $c = 6\%$ of the “aeerr” case approximates a MAPE of $c = 14\%$ for the constant case. In this example the difference of 8% results in significant capacity size i.e. of $c = (2.7\text{GWh}/365) * 0.08 \approx 580\text{kWh}$. Therefore, [Figure 12](#) can provide critical hints towards the efficiency assessment of a variable storage (e.g. if capacity of connected EVs is considered), or how it should be sized on its intra-day requirements.

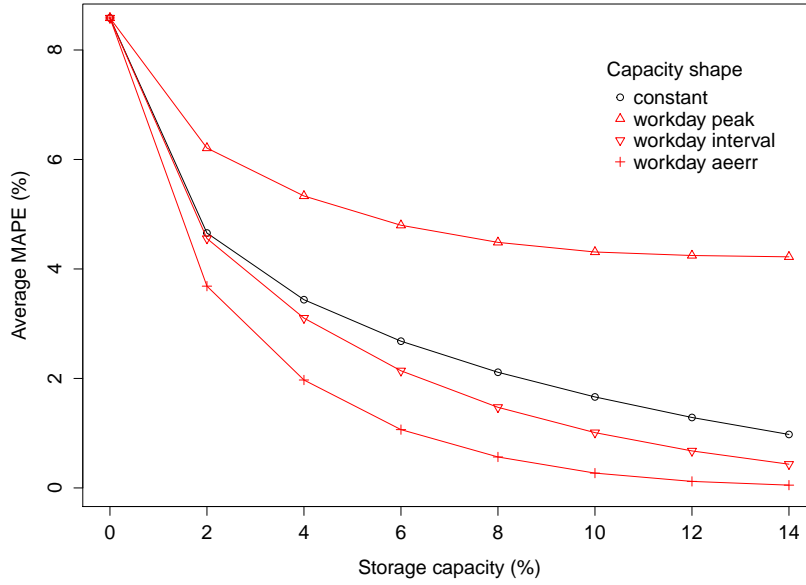


Fig. 12 Improvement rate of the absorbed forecast errors for the selected storage shapes

7 Conclusions and Future Work

As existing buildings are getting equipped with the more stochastic energy generation and consumption assets such as solar panels, EVs etc., the forecast accuracy will play an increasingly important role in taking informed business decisions. Understanding the errors in the energy signature prediction of a facility is important for taking actions to reduce and measure their impact [9]. Doing so may result on business advantages and enable better cost-managing measures, participation in demand-response programmes, or even new business opportunities in the envisioned smart grid era such as energy trading.

We have presented here an approach that focuses on understanding propagation of the forecast error, and its role in estimating storage capacity requirements. The SARIMA model is used to investigate an efficient storage distribution to absorb the propagating forecasting errors. It is shown how the dynamic behaviour provokes higher errors, and assessed in a step-wise manner how the deployment of (variable) storage could assist towards absorbing them. We have not explicitly identified the nature of this storage, i.e. if it is static or dynamic, as this will depend on the available assets (e.g. existence of EVs), strategic decisions, sustainability goals, economic analysis and other factors that are outside of the scope of this work.

Although an empirical approach is provided, tools could be developed to automate the steps and adjust it to the characteristics of the individual infrastructure. Hence, the development of intelligent algorithms considering not only impact on the technical side, but also on the business one, seem promising

towards developing sustainable strategies and managing future energy infrastructures as an ecosystem [2]. Identification of case-specific patterns may lead to potentially better estimation of storage requirements and the role existing and future company assets.

Acknowledgment

The authors would like to thank the European Commission for their support and the partners of the EU FP7 project SmartKYE (www.SmartKYE.eu) for the fruitful discussions.

References

1. IFMA Foundation, *Technology for Facility Managers: The Impact of Cutting-Edge Technology on Facility Management*, E. Teicholz, Ed. John Wiley & Sons, Somerset, NJ, USA, Sep. 2012.
2. D. Ilić, S. Karnouskos, P. Goncalves Da Silva, and S. Detzler, “A system for enabling facility management to achieve deterministic energy behaviour in the smart grid era,” in *3rd International Conference on Smart Grids and Green IT Systems (SmartGreens), Barcelona, Spain*, 3–4 Apr. 2014.
3. J. Mathieu, P. Price, S. Kiliccote, and M. Piette, “Quantifying changes in building electricity use, with application to demand response,” *Smart Grid, IEEE Transactions on*, vol. 2, no. 3, pp. 507–518, Sep. 2011.
4. S. Lamparter, S. Becher, and J.-G. Fischer, “An agent-based market platform for smart grids,” in *Proceedings of the 9th International Conference on Autonomous Agents and Multiagent Systems: Industry track*, ser. AAMAS '10. Richland, SC: International Foundation for Autonomous Agents and Multiagent Systems, 2010, pp. 1689–1696. [Online]. Available: <http://portal.acm.org/citation.cfm?id=1838194.1838197>
5. S. Karnouskos, “Demand side management via prosumer interactions in a smart city energy marketplace,” in *IEEE International Conference on Innovative Smart Grid Technologies (ISGT 2011), Manchester, UK*, Dec. 5–7 2011.
6. European Commission, “SmartGrids SRA 2035 – Strategic Research Agenda,” European Technology Platform SmartGrids, European Commission, Tech. Rep., Mar. 2012. [Online]. Available: <http://www.smartgrids.eu/documents/sra2035.pdf>
7. R. Sevlian and R. Rajagopal, “Value of aggregation in smart grids,” in *Smart Grid Communications (SmartGridComm), 2013 IEEE International Conference on*, 2013, pp. 714–719.
8. D. Backer, “Power quality and asset management the other ”two-thirds” of AMi value,” in *Rural Electric Power Conference, 2007 IEEE*, May 2007, pp. C6 –C6–8.
9. M. L. Goldberg and G. K. Agnew, “Measurement and verification for demand response,” DNV KEMA Energy and Sustainability, Tech. Rep., Feb 2013.
10. D. Ilić, P. Goncalves da Silva, S. Karnouskos, and M. Jacobi, “Impact assessment of smart meter grouping on the accuracy of forecasting algorithms,” in *Proceedings of the 28th Annual ACM Symposium on Applied Computing (SAC)*, ser. SAC '13. New York, NY, USA: ACM, 2013, pp. 673–679. [Online]. Available: <http://doi.acm.org/10.1145/2480362.2480491>
11. D. Ilić, S. Karnouskos, and P. Goncalves da Silva, “Improving load forecast in prosumer clusters by varying energy storage size,” in *IEEE Grenoble PowerTech 2013, Grenoble, France*, 16 – 20 Jun. 2013.
12. PJM, “PJM Manual 18: PJM Capacity Market,” PJM (www.pjm.com), Tech. Rep., Nov. 2013. [Online]. Available: <http://www.pjm.com/~media/documents/manuals/m18.ashx>

13. F. Genoese and M. Genoese, "Assessing the value of storage in a future energy system with a high share of renewable electricity generation," *Energy Systems*, pp. 1–26, 2013.
14. K. Divya and J. Østergaard, "Battery energy storage technology for power systems – an overview," *Electric Power Systems Research*, vol. 79, no. 4, pp. 511 – 520, 2009. [Online]. Available: <http://www.sciencedirect.com/science/article/pii/S0378779608002642>
15. V. Alimisis and N. Hatziaargyriou, "Evaluation of a hybrid power plant comprising used EV-batteries to complement wind power," *Sustainable Energy, IEEE Transactions on*, vol. 4, no. 2, pp. 286–293, 2013.
16. T. M. Peng, N. Hubele, and G. Karady, "Advancement in the application of neural networks for short-term load forecasting," *Power Systems, IEEE Transactions on*, vol. 7, no. 1, pp. 250–257, 1992.
17. M. Cho, J. C. Hwang, and C.-S. Chen, "Customer short term load forecasting by using arima transfer function model," in *Energy Management and Power Delivery, 1995. Proceedings of EMPD '95., 1995 International Conference on*, vol. 1, 1995, pp. 317–322vol.1.
18. S. Zhu, J. Wang, W. Zhao, and J. Wang, "A seasonal hybrid procedure for electricity demand forecasting in china," *Applied Energy*, vol. 88, no. 11, pp. 3807–3815, 2011. [Online]. Available: <http://www.sciencedirect.com/science/article/pii/S0306261911002960>
19. P. Pinson, G. Papaefthymiou, B. Klockl, and J. Verboomen, "Dynamic sizing of energy storage for hedging wind power forecast uncertainty," in *Power Energy Society General Meeting, 2009. PES '09. IEEE*, 2009, pp. 1–8.
20. P. Sanchez-Martin, G. Sanchez, and G. Morales-Espana, "Direct load control decision model for aggregated EV charging points," *Power Systems, IEEE Transactions on*, vol. 27, no. 3, pp. 1577–1584, 2012.